

Quasicrystals: Atomic coverings and windows are dual projects.

Peter Kramer

Institut für Theoretische Physik der Universität
Tübingen, Germany.

7th February 2008

Abstract.

In the window approach to quasicrystals, the atomic position space E_{\parallel} is embedded into a space $E^n = E_{\parallel} + E_{\perp}$. Windows are attached to points of a lattice $\Lambda \in E^n$. For standard 5fold and icosahedral tiling models, the windows are perpendicular projections of dual Voronoi and Delone cells from Λ . Their cuts by the position space E_{\parallel} mark tiles and atomic positions. In the alternative covering approach, the position space is covered by overlapping copies of a quasi-unit cell which carries a fixed atomic configuration. The covering and window approach to quasicrystals are shown to be dual projects: D - and V -clusters are defined as projections to position space E_{\parallel} of Delone or Voronoi cells. Decagonal V -clusters in the Penrose tiling, related to the decagon covering, and two types of pentagonal D -clusters in the triangle tiling of 5fold point symmetry with their windows are analyzed. They are linked, cover position space and have definite windows. For functions compatible with the tilings they form domains of definition. For icosahedral tilings the V -clusters are Kepler triacontahedra, the D -clusters are two icosahedra and one dodecahedron.

1 Introduction: Windows versus coverings.

The standard approach for quasicrystal structure uses the project of *atomic windows*: These are polytopes with centers located at points of the unit cell from a lattice Λ in an embedding space $E^n = E_{\parallel} + E_{\perp}$. Atoms are then located on position space E_{\parallel} by parallel cuts through the windows, compare

Katz and Gratias [8, 9] for icosahedral examples. The alternative project of *coverings* in quasicrystals was introduced by Gummelt [6], based on earlier concepts due to Burkov [3] and Conway [4]. The Penrose tiling was interpreted in [6] as a system of decagonal covering clusters with overlaps. These clusters were related to the concept of a *quasi-unit cell* by Jeong, Steinhardt et al. [16, 17, 18]. The full quasicrystal structure is then composed from overlapping atomic configurations on copies of the quasi-unit cell. Moreover, Steinhardt et al. interpret these atomic configurations from the point of view of local energy. This interpretation takes up earlier work by Janot [7]. For a comment we refer to Urban [19].

What is the relation of the projects of coverings and windows to one another? What are the covering clusters and links for a given tiling? What is the meaning of a (quasi-) unit cell of a quasicrystal whose points, in contrast to crystals, are not related by the action of a translation group? In the present paper we try to answer these structure questions. We confront both projects from the point of view of an embedding space, a lattice, its Voronoi cells V , its dual Delone cells D^a, D^b, \dots [5], and corresponding tilings. The Voronoi and Delone cells of the lattice in the embedding space are the basis for a set of canonical tilings [10]: The windows for these tilings are perpendicular projections of Voronoi or Delone cells.

We shall show that windows and coverings are dual projects. We define and analyze *clusters as projections to position space of Delone or Voronoi cells* $D_{\parallel}^a, D_{\parallel}^b, \dots$ or V_{\parallel} . We term them *D-clusters or V-clusters* respectively. We determine *domains of definition for functions on quasiperiodic tilings* and show that they can be related to sets of *V-clusters* or *D-clusters*. These concepts are introduced and illuminated in section 2 with the Fibonacci tiling, projected from the square lattice, and in section 3 with a tiling projected from the lattice A_2 . In section 4 we determine for the Penrose-Robinson tiling, projected from the lattice A_4 [2], its *V-clusters* and obtain the decagon covering of Gummelt [6]. In section 5 we construct for the triangle tiling, dually projected from the lattice A_4 [2], two pentagonal D^a, D^b -clusters and the covering. In section 6 we sketch the clusters for dual icosahedral tilings. The *V-clusters* from the primitive and *F*-lattice are Kepler triacontahedra, the three *D-clusters* from the *F*-lattice are icosahedra or dodecahedra.

2 Clusters from Delone cells in the Fibonacci tiling.

Fibonacci tiling and klotz construction.

Consider the Fibonacci tiling constructed from the square lattice Λ of edge length s in E^2 by duality [11]. Its Voronoi cells $V(q)$ are squares centered at all lattice points q . Its dual Delone cells D are squares centered at all vertices of the Voronoi cells. All Delone cells belong to a single translation orbit. A 2D fundamental domain \mathcal{F} in E^2 under the action of Λ is provided by a single Voronoi cell V or, equivalently, by a single Delone cell D . The 1-boundaries P of a Voronoi cell are its four edge lines. The dual 1-boundaries P^* of a Delone cell are its four edge lines. Pairs P, P^* of dual 1-boundaries intersect in midpoints of the edges of the squares. Define the decomposition $E^2 = E_{\parallel} + E_{\perp}$ in the usual fashion: x_{\parallel} runs, w.r.t. to a densest lattice plane of Λ along a line of slope τ^{-1} , $\tau = (1 + \sqrt{5})/2$ respectively. The *klotz construction* [13] for the Fibonacci tiling [11] arises as follows: For each intersecting pair P, P^* , form at its intersection point the convex klotz cells $P_{\perp} \oplus P_{\parallel}^*$. The two klotz cells (A, B) , see Fig.1, are two squares (A, B) of edge length $|L| = \tau|S|$, $|S| = s/\sqrt{\tau + 2}$ respectively, with boundaries perpendicular or parallel to E_{\parallel} . Any line with points $x = x_{\parallel} + c_{\perp}$, $-\infty < x_{\parallel} < \infty$ intersects the klotz construction in a Fibonacci tiling \mathcal{T}^* with the tiles $(L := A_{\parallel}, S := B_{\parallel})$. A window for the full local isomorphism class of all tilings \mathcal{T}^* may be taken as a perpendicular interval of length $|L| + |S|$ centered at a lattice point q . This interval is the perpendicular projection $V_{\perp}(q)$ of the Voronoi cell and appears in the klotz construction at all positions of lattice points q .

Quasiperiodic functions and fundamental domains.

Atomic densities or electronic potentials in quasicrystals require functional analysis on the position space. We recall the following relations on E^n : Under the geometric group action of $q \in \Lambda$, $x, x' \in E^n$, $(q, x) \rightarrow x' = x + q$, a *fundamental domain* is a subset $\mathcal{F} \in E^n$ which has exactly one point from each translation orbit. The geometric group action yields for functions f on E^n the group operators $T_q : f(x) \rightarrow (T_q f)(x) := f(x - q)$. Suppose now that f is periodic on E^n modulo Λ . We define a fundamental domain for f as a subset $\mathcal{F} \in E^n$ such that any value of f on $E^n - \mathcal{F}$ is obtained by the group action. Clearly a fundamental domain for a periodic function f can be identified with a *fundamental domain* for the geometric action of Λ .

1 Prop. Two klotz cells (A, B) form a *fundamental domain \mathcal{F} for functions f on E^2 periodic modulo Λ* .

Proof: The pairs of dual boundaries underlying the cells (A, B) are representatives of different translation orbits under Λ . The cells do not overlap and together have the same volume as the Voronoi square.

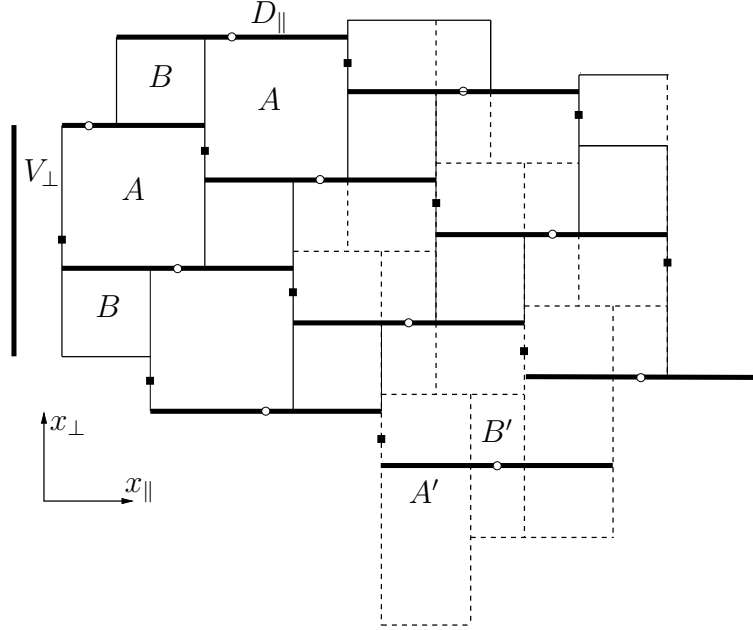


Fig. 1 The square lattice Λ of edge length s in E^2 has Voronoi squares $V(q)$, centered at lattice points q (full squares), and Delone squares D , centered at Voronoi vertices (open circles). The lattice admits a periodic tiling into two squares (A, B) of edge lengths $|L| = \tau|S|, |S|$, called klotz cells and shown on the left-hand side. The edges of these squares run along directions x_{\parallel} horizontal, x_{\perp} vertical of slope τ^{-1}, τ with respect to a densest lattice line. A pair (A, B) of two such squares form a fundamental domain \mathcal{F} for the lattice. The intersection of a parallel line with the two squares (A, B) forms a Fibonacci tiling \mathcal{T}^* with tiles $L = A_{\parallel}, S = B_{\parallel}$. The window of the tiling is $V_{\perp}(q)$ centered at lattice points q . Its size is indicated by a perpendicular bar on the left-hand side. The Delone projections D_{\parallel} to position space E_{\parallel} centered at Voronoi vertices (heavy lines at open circles) provide fundamental domains for functions compatible with the Fibonacci tiling. They bound pairs $A \cup B$ and $B \cup A$ from below and above. On parallel line sections they give rise to D -clusters (LS) or (SL). A second periodic tiling in E^2 with two rectangles (A', B') is shown on the lower right-hand side (dashed lines). Its intersection with a horizontal line $x = x_{\parallel} + c_{\perp}$, $-\infty < x_{\parallel} < \infty$, yields a deflated Fibonacci tiling $\mathcal{T}_{\tau^{-1}}^*$ with tiles (L', S') of length scaled by the factor τ^{-1} .

τ^{-1} . The union of the two tilings is shown in the middle part. In the parallel subtiling from this union, any cluster $(LS), (SL)$ of \mathcal{T}^* gets the symmetric subdivision $(L'S'L')$, and consecutive clusters are disjoint or linked by a tile L' .

Quasiperiodic functions on a parallel line section are characterized as follows: Take a function f , defined by its values on the two cells (A, B) (or on any other equivalent fundamental domain) \mathcal{F} , and repeated on E^2 modulo Λ . The restriction of f to its values on a line $x = x_{\parallel} + c_{\perp}, -\infty < x_{\parallel} < \infty$ gives rise to a quasiperiodic function on this line. The *fundamental domain for a quasiperiodic function* that determines its value everywhere on the 1D horizontal line is seen in the embedding space E^2 as a 2D fundamental domain w.r.t. the action of Λ .

Quasiperiodic functions of this general type do not take the same values on different passages of the line through A or through B , and so they are not compatible with the Fibonacci tiling \mathcal{T}^* . The class of quasiperiodic functions f *compatible with the tiling \mathcal{T}^** on the line E_{\parallel} must have the following restricted property, as discussed for example in [11]: On each of the two chosen klotz cells (A, B) , its values must be *independent of x_{\perp}* . These values by repetition under Λ generate on any parallel line section a quasiperiodic function which takes the same values on each passage through A or B . We refer to Arnold [1] for a discussion of quasiperiodic functions along similar lines.

2 Def. Let the tiling \mathcal{T} consist of a minimal finite set $\langle p_i \rangle \in E_{\parallel}$ of prototiles p_i and their translates appearing in \mathcal{T} . A *fundamental domain for a quasiperiodic function f on E_{\parallel} compatible with the tiling* is a subset of points $x_{\parallel} \in E_{\parallel}$ which contains one and only one translate in \mathcal{T} of any point from any prototile. A fundamental domain with this property will be denoted by $\mathcal{F}(\mathcal{T}, \Lambda)$. It depends on the tiling \mathcal{T} , the lattice Λ , and the projection $E^n = E_{\parallel} + E_{\perp}$. The volume of the fundamental domain is $|\mathcal{F}(\mathcal{T}, \Lambda)| = \sum_i |p_i|$. For the Fibonacci tiling we find:

3 Prop. The fundamental domain $\mathcal{F}(\mathcal{T}^*, \Lambda)$ for any function f compatible with the Fibonacci tiling \mathcal{T}^* , can be taken as a line interval in E_{\parallel} of length $|L| + |S|$, consisting of a short and a long interval of the tiling \mathcal{T}^* . The values of f on the two intervals are then extended on each klotz cell (A, B) to a 2D function independent of x_{\perp} . By repetition modulo Λ and intersection with a parallel line they give rise to a particular quasiperiodic function.

Linked D -Clusters.

The parallel projections D_{\parallel} of the Delone squares are line sections of length $|L| + |S|$. These projections appear in the klotz tiling at the Delone centers. Each one separates a pair (B, A) on top from a pair (A, B) of klotz cells at the bottom. The boundary line itself we assign for uniqueness to the top pair of klotz cells. If a horizontal intersection line passes the top or bottom pair, any one of the two cuts provides a fundamental domain $\mathcal{F}(\mathcal{T}^*, \Lambda)$. Both the (SL) and the (LS) combination we term a D -cluster.

4 Prop. The Fibonacci tiling $(\mathcal{T}^*, (L, S))$ is equivalent to a chain of linked D -clusters of type (LS), (SL). The clusters can be locally determined: Each one is equivalent to the parallel projection D_{\parallel} of a Delone cell and forms a fundamental domain $\mathcal{F}(\mathcal{T}^*, \Lambda)$. Consecutive clusters are disjoint or linked by a tile S in the form $(L(S)L)$.

Proof: Compare Fig.1. In the tiling \mathcal{T}^* , form disjoint clusters from all consecutive strings (LS) except for the string (LSLLS). This string is interpreted with three clusters as $(L(S)L)(LS)$, with the first two clusters linked by the tile S .

Symmetric subtiling and windows for D -clusters.

The D -clusters as parallel projections D_{\parallel} carry the two alternative subtilings (LS), (SL). We can remove this asymmetry by use of the deflated subtiling $\mathcal{T}_{\tau^{-1}}^*$. Its new rectangular klotz cells (A', B') in E^2 are shown with dashed lines in the lower part of Fig.1. The deflated tiles from parallel sections are $(L', S') = \tau^{-1}(L, S)$. In the union of the original and deflated tiling, all projections D_{\parallel} and hence all D -clusters get the symmetric subtiling (LS), (SL) $\rightarrow (L'S'L')$. From the point of view of the deflated tiling, all strings $(L'L')$ separate disjoint clusters, all strings $(S'L'S')$ mark consecutive clusters linked by a tile L' . Note that the D -clusters are not fundamental domains with respect to the deflated tiling! So far we have not implemented the action of the point group, generated here by inversion, on functions f . This would require restricting their domain to the counterpart of the asymmetric unit in the terminology of periodic crystallography.

The deflated tiling $\mathcal{T}_{\tau^{-1}}^*$ allows us to determine the *window for centers of D -clusters*: The centers correspond to the midpoints of its tiles S' . Therefore their windows are the projections B'_{\perp} of length $|L|$ of the rectangles B' , centered at the vertices of Voronoi cells in Fig. 1.

3 V -Clusters in a tiling with the lattice A_2 .

The klotz construction uses the duality between Voronoi and Delone cells for a single lattice. For illustration of duality we choose the root lattice A_2 in E^2 . Its Voronoi cells V are hexagons centered at lattice points, its Delone cells are two types of triangles D^a, D^b centered at two different translation classes of vertex points of V . These cells are shown in the top part of Fig. 2.

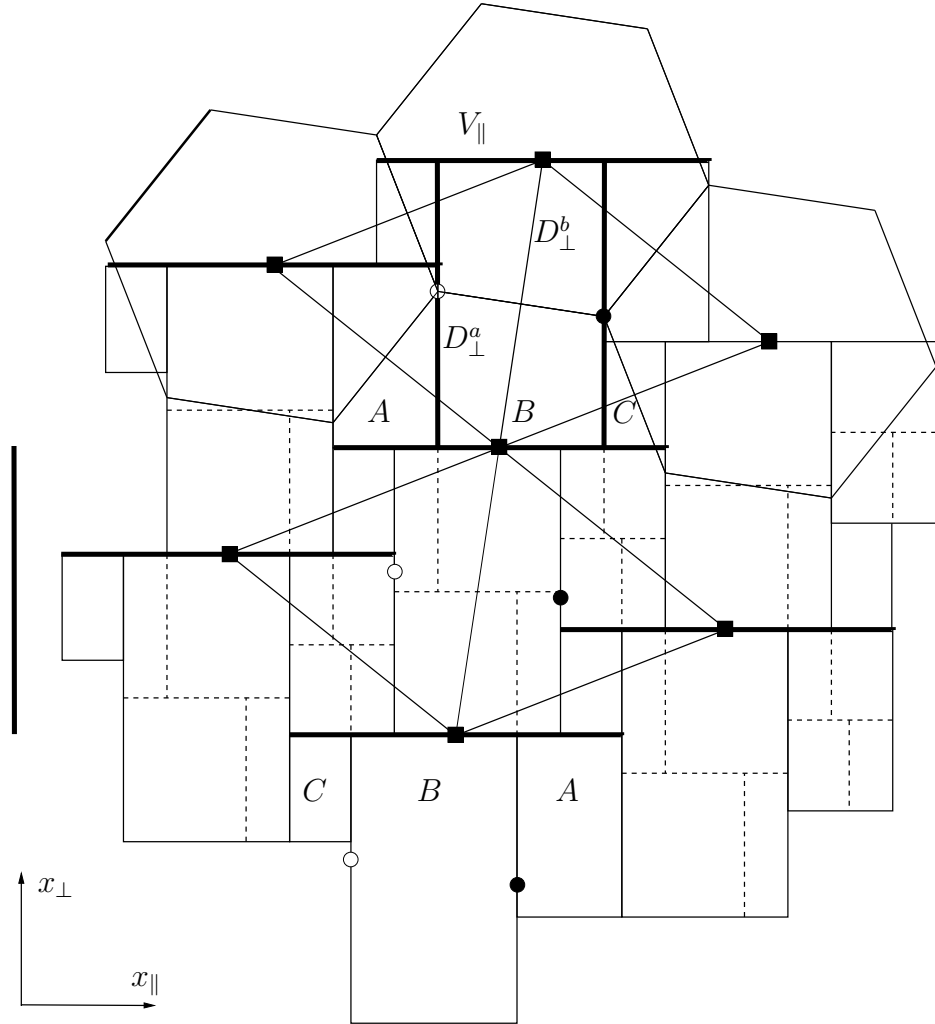


Fig. 2. The root lattice A_2 . Its Voronoi cells $V(q)$ are hexagons centered at lattice points q (full squares), its Delone cells D^a, D^b form two translation orbits of triangles centered at vertices of V (open and full circles). They are shown in the top part. The three rectangular klotz cells A, B, C shown in the middle and bottom part arise from a decomposition $E^2 = E_{\parallel} + E_{\perp}$. The tiling \mathcal{T} has the tiles $A_{\parallel}, B_{\parallel}, C_{\parallel}$. Its window consists of two projections

D_{\perp}^a, D_{\perp}^b centered at vertices of V . The size of the window is indicated on the left-hand side by a perpendicular bar. The parallel projections V_{\parallel} of Voronoi cells (heavy lines) at lattice points q bound triples $A \cup B \cup C$ from below and $C \cup B \cup A$ from above. On parallel line sections they produce the V -clusters as $(A_{\parallel} B_{\parallel} C_{\parallel})$ or $(C_{\parallel} B_{\parallel} A_{\parallel})$. Both form domains of definition for quasiperiodic functions f compatible with the tiling. Consecutive V -clusters are linked by tiles A_{\parallel} or C_{\parallel} . A subdivision of the klotz cells A, B is marked in the middle part by dashed lines. It yields an inversion-symmetric identical subtiling of the two clusters.

Two dual tilings arise from a fixed decomposition $E^2 = E_{\parallel} + E_{\perp}$: In \mathcal{T} the windows are projections D_{\perp}^a, D_{\perp}^b of Delone cells, in \mathcal{T}^* they are projections V_{\perp} of Voronoi cells. We choose \mathcal{T} since it is in analogy to the projection of the Penrose tiling in section 4. Three klotz cells A, B, C are shown at the bottom of Fig. 2. Their projections form the tiles $A_{\parallel}, B_{\parallel}, C_{\parallel}$. The parallel projections V_{\parallel} of Voronoi cells centered at lattice points yield one type of V -clusters as the strings $(A_{\parallel} B_{\parallel} C_{\parallel})$ or $(C_{\parallel} B_{\parallel} A_{\parallel})$. Both form *domains of definition* $\mathcal{F}(\mathcal{T}, A_2)$ for quasiperiodic functions f compatible with the tiling. Consecutive V -clusters are linked by the tiles A_{\parallel} or C_{\parallel} . The klotz cells (A, B) may again be subdivided by dashed lines as indicated in the middle part of Fig. 2. This subdivision provides a subtiling of both V -clusters which is symmetric under local inversion.

4 Decagonal V -clusters in the Penrose-Robinson tiling from the lattice A_4 .

We first summarize the construction of the decagon covering due to Gummelt [6]. It uses the Penrose tiling \mathcal{T} with rhombus edge length s and Robinson decomposition together with the deflated tiling $\mathcal{T}_{\tau^{-1}}$ with edge length $\tau^{-1}s$ again with Robinson decomposition. Select in $\mathcal{T}_{\tau^{-1}}$ all the vertex configurations **king** and mark in each one a center point, Fig. 3. From the empire of **king** it can be shown that a decagon of edge length s is forced around the center point, with a unique subdivision called the cartwheel [4]. It is shown by Gummelt [6] that these cartwheel decagons yield a *covering* which is equivalent to the Penrose tiling.

We employ the deflation sequence of tilings $\mathcal{T}_{\tau} \rightarrow \mathcal{T} \rightarrow \mathcal{T}_{\tau^{-1}}$, compare also [16], to redescribe the decagons according to Fig. 3. We start with a thick rhombus in the first tiling. On it we mark a point with a full square. The first deflation yields in \mathcal{T} the vertex configuration **jack**. The next deflation

yields in $\mathcal{T}_{\tau-1}$ the vertex configuration **king**. This **king** in Robinson subdivision enforces the cartwheel decagon of edge length s . The marked point is maintained in the three steps. It follows from this sequence of deflations that *the decagon centers are fixed at the marked points on all the thick rhombus tiles of \mathcal{T}_τ* .

Turn to the method of windows and projection. We follow [2] and project the Penrose tiling of type \mathcal{T} from the root lattice A_4 . The embedding space E^4 for this lattice splits into two 2D spaces E_{\parallel}, E_{\perp} of 5fold symmetry. There are four Delone cells whose perpendicular projections up to inversion form a small and a large pentagon. Their centers form four translation orbits of Voronoi vertices. The Voronoi vertices are called the deep and shallow holes [5] in the lattice Λ . We denote representatives of the two shapes of Delone cells by D^a, D^b and their projections by D_{\perp}^a, D_{\perp}^b . Their centers are shallow and deep holes respectively. Together with their mirror images they form the windows for the Penrose tiling. The klotz cells are formed from 10 pairs of dual 2D boundaries which represent different translation orbits. Similar as in the Fibonacci projection it can be shown that these 10 klotz cells form a fundamental domain under A_4 . The Penrose tiles are rhombic projections P of 2D boundaries from the Voronoi cell. Their duals P^* are acute and obtuse triangles, projections of 2D boundaries from the Delone cells. A *vertex configuration* of Penrose tiles is coded by an overlap of the dual coding triangles inside a Delone window [2]. In the notation of [2], the vertex configurations 1 – 3 are coded in the small pentagon D_{\perp}^a , the vertex configurations 5 – 8 in the large pentagon D_{\perp}^b . Turn then to the projections V_{\parallel} and to the V -clusters.

5 Prop. The (linked) V -clusters of the Penrose-Robinson tiling are decagonal projections V_{\parallel} to position space of edge length s . Two decagons form a fundamental domain $\mathcal{F}(\mathcal{T}, A_4)$.

The projection is in shape equal to the window V_{\perp} of the dual triangle tiling, see section 5. For the Penrose tiling, a fundamental domain $\mathcal{F}(\mathcal{T}, A_4)$ according to Def. 2 should contain 10 thick and 10 thin rhombus tiles. A single decagonal V_{\parallel} -cluster of edge length s can cover 5 thick and 5 thin rhombus tiles. Therefore not one, but two decagonal V_{\parallel} -clusters, rotated by an angle $2\pi/10$ to one another, are required to form $\mathcal{F}(\mathcal{T}, A_4)$. Both orientations occur in the decagon covering and from Fig. 4 are related to the orientations of thick rhombus tiles from (\mathcal{T}_τ, A_4) .

We wish to locate the centers of these decagons by the projection method. This can be done with the help of selected vertex configurations as follows: In the coding of the vertex configurations inside the small and large pentagons D_{\perp}^a, D_{\perp}^b , we look for *vertex configurations from coding triangles which share a single vertex of D_{\perp}^a or D_{\perp}^b* . Dualization of boundaries [13] implies that the

tiles of such a vertex configuration *must belong to a single Voronoi cell*. This condition holds true for the vertex configuration 2, the **jack** coded in D_{\perp}^a , and for vertex configuration 6, the **king** coded in D_{\perp}^b . Any king in the tiling forces a jack with the same projected lattice point q_{\parallel} , and so we can restrict the analysis to jacks.

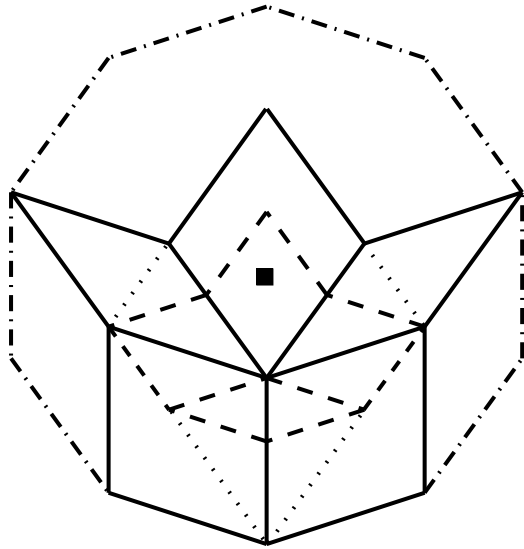


Fig. 3. The Penrose tiling (\mathcal{T}, A_4) , its inflation by τ : (\mathcal{T}_τ, A_4) and its deflation by τ^{-1} : $(\mathcal{T}_{\tau^{-1}}, A_4)$. At a projected point q_{\parallel} (full square) from the lattice A_4 , a thick rhombus tile of (\mathcal{T}_τ, A_4) (dotted lines) converts first into a jack of (\mathcal{T}, A_4) (full lines) and then into a king of $(\mathcal{T}_{\tau^{-1}}, A_4)$ (dashed lines). The empire of the king in Robinson decomposition forces the cartwheel decagon (--- line) of Conway and Gummelt. The decagons are V -clusters, two of them form a fundamental domain for functions f compatible with the Penrose tiling.

We have then arrived from the V -clusters in the projection method at the decagons of Gummelt [6] with the following qualifications:

6 Prop.

- (i) The V -clusters V_{\parallel} of the Penrose tiling of edge length s , located at projected lattice points q_{\parallel} in the vertex configurations **jack**, coincide with the decagons of Gummelt [6].
- (ii) Two decagons of edge length s form a fundamental domain $\mathcal{F}(\mathcal{T}, A_4)$ for functions f compatible with the Penrose tiling of the same edge length, not with any of its inflations or deflations.

- (iii) The decagon edges around projected lattice points q_{\parallel} on **jacks**, Fig. 4, do not always appear as part of the rhombus tiling. The different decagonal domains of the covering become identical with the cartwheel upon subdivision by deflation to $(\mathcal{T}_{\tau^{-1}}, A_4)$.
- (iv) The decagon centers are fixed to projected lattice points q_{\parallel} on the thick rhombus tiles of the inflated tiling $(\mathcal{T}_{\tau}, A_4)$. Their windows are, up to perpendicular shifts from the rhombus vertex to the lattice point, the acute triangles inside the Delone windows for this tiling.

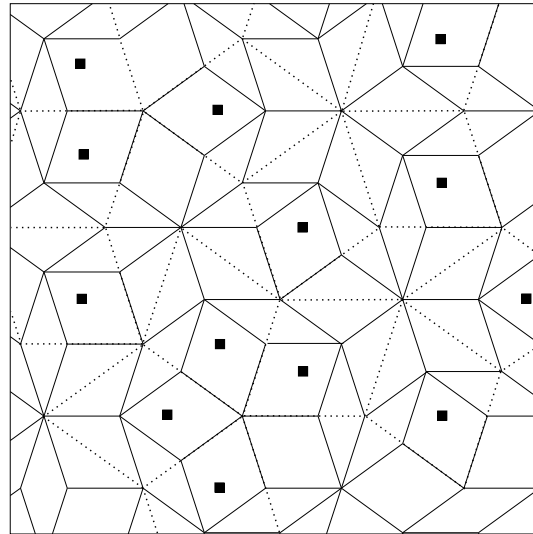


Fig. 4. Part of a Penrose tiling. Projected lattice points q_{\parallel} are marked by full squares. They are centers of decagonal V -clusters and cartwheel decagons at jack vertex configurations, compare Fig. 3. These points are also located on the thick rhombus tiles (dotted lines) of the inflated Penrose tiling.

The links between V -clusters are clearly related to the sharing of (parallel projected) dual boundaries. The window technique allows to characterize the linkage and the relative frequencies and to compare with [6].

5 Pentagonal D -clusters in the triangle tiling from the lattice A_4 .

The triangle tiling [2] is the dual tiling \mathcal{T}^* from the lattice A_4 . The Voronoi and Delone cells are the same as for the Penrose tiling, but the projections interchange their role. Its window is a decagon V_{\perp} . Its tiles are an acute and

an obtuse golden triangle, coded in E_\perp by Penrose rhombus tiles. There are 9 vertex configurations.

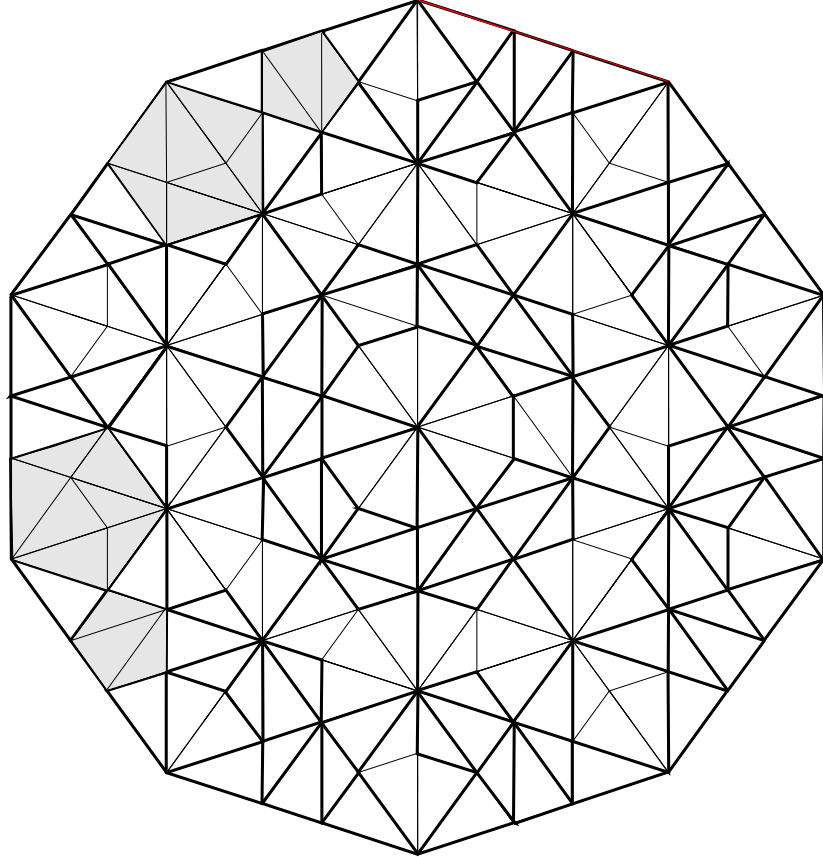


Fig. 5. Part of a triangle tiling (\mathcal{T}^*, A_4) . The small and large pentagons (heavy edge lines) mark the linked Delone $D_{\parallel}^a, D_{\parallel}^b$ -clusters which cover the tiling by triangles (weak edge lines if not edge of a pentagon). The four grey pentagons together form a fundamental domain of definition $\mathcal{F}(\mathcal{T}^*, A_4)$ for functions compatible with the triangle tiling. They comprise the two triangles each in 10 orientations.

7 Prop. The $D_{\parallel}^a, D_{\parallel}^b$ -clusters of the triangle tiling are two types of linked pentagons. Together with their mirror images they form a fundamental domain $\mathcal{F}(\mathcal{T}^*, A_4)$ for the triangle tiling. These Delone clusters form a covering of the triangle tiling.

Proof: To determine configurations of triangles belonging to D -clusters we select codings for vertex configurations by Penrose tiles in the decagon which share a single (shallow or deep hole) vertex of the Voronoi cell. It turns out

that, in the enumeration of [2], the vertices 4, 5, 6, 7 produce small pentagonal D_{\parallel}^a -clusters and the vertex 2 produces large D_{\parallel}^b -clusters. These two types of pentagons are linked and yield a covering of the triangle pattern as shown in Fig. 5. The windows for the two pentagons can be found from the combination of vertex windows as shown in Fig. 6. Projections of shallow and deep holes are marked as full and white circles. More details of the Delone windows are given in appendix A. The proof of the covering property from the projection and window method is given in appendix B. \square

The triangle tiling is applied to decagonal $AlCuCo$ in [15]. The implications of linked pentagonal D -clusters in terms of shared dual boundaries should be studied.

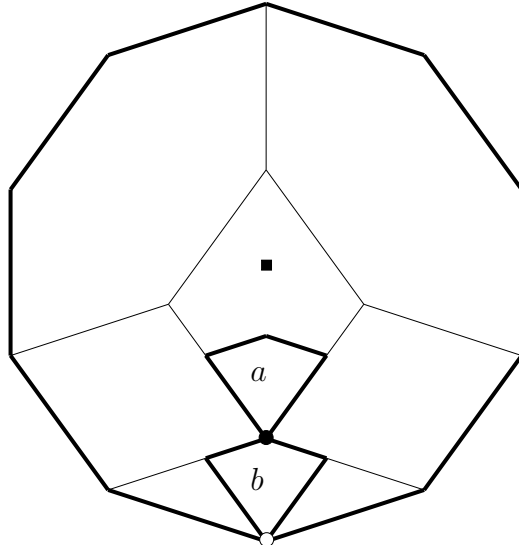


Fig. 6. The windows $w(D^a), w(D^b)$ for the small and large pentagonal D -clusters in the triangle tiling are two regions marked (a, b) in the decagonal window $V_{\perp} \in E_{\perp}$ modulo 5fold rotations. For details of the construction compare appendix A.

6 V - and D -clusters in icosahedral tilings.

The three icosahedral modules P, F, I can be projected from the P, F, I centered hypercubic lattice in E^6 . All known icosahedral tilings are related to the canonical ones based on duality. From the analysis of the canonical icosahedral tilings [10, 14] for the P, F lattices one can immediately draw the following conclusion on the shape of the V - and D -clusters in position space:

P lattice: The Voronoi and Delone cells of the hypercubic lattice coincide in shape and so do their projections. The tiles are the well-known thick

and thin rhombohedra of edge length ⑤. Both the windows V_{\perp} and the D -clusters D_{\parallel} are the triacontahedra of Kepler with edge length ⑤. From the translation orbits [12] one can explore their relation to the fundamental domain $\mathcal{F}(\mathcal{T}^*, P)$.

F lattice: The lattice F has three different translation orbits of Delone cells denoted as D^a, D^b, D^c . In the tiling (\mathcal{T}^*, F) , the window V_{\perp} is again the triacontahedron of Kepler of edge length ⑤. The tiles are six tetrahedra projected from 3-boundaries of the Delone cells. The vertex configurations were studied in [14]. This tiling is used for modelling atomic positions of *AlPdMn* and is closely related to the approach of Katz and Gratias [8, 9]. From the present analysis we get three Delone clusters $D_{\parallel}^a, D_{\parallel}^b, D_{\parallel}^c$. Two of them are icosahedra with the edge lengths ②, $\tau\text{②}$, where $\text{②} = \frac{2}{\sqrt{\tau+2}}\text{⑤}$, one is a dodecahedron of edge length ②, see Fig. 7. The windows for these Delone D -clusters and their relation to the fundamental domain $\mathcal{F}(\mathcal{T}^*, F)$ must be analyzed.

In the dual tiling (\mathcal{T}, F) , the three Delone windows are $D_{\perp}^a, D_{\perp}^b, D_{\perp}^c$. The tiles are two rhombohedra and four pyramids projected from 3-boundaries of the Voronoi domains. The Voronoi clusters V_{\parallel} are Kepler triacontahedra related to the fundamental domain $\mathcal{F}(\mathcal{T}, F)$.

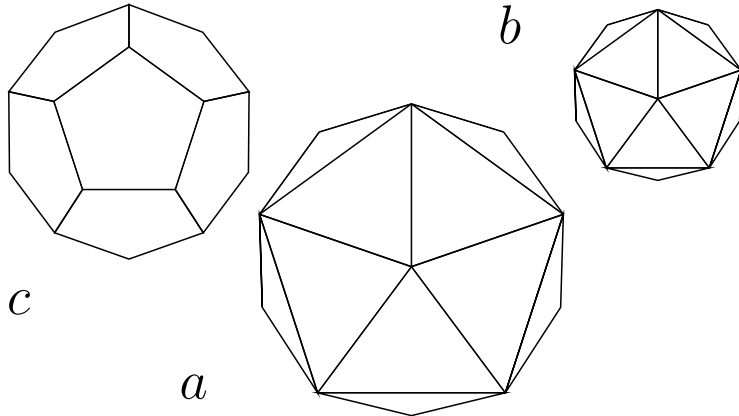


Fig. 7. Schematic view of the three Delone D -clusters for the icosahedral tiling (\mathcal{T}^*, F) : The three Delone D^a, D^b, D^c -clusters are a dodecahedron and two icosahedra.

Structure questions to be studied are the fundamental domain and covering property, the linkage of V, D -clusters in relation to the modules and shared dual boundaries, their local point symmetry, and atomic positions on them. In all cases the technique of windows for the tilings, the tiles and vertex

configurations, and for atomic positions is available. It allows to implement the project of D - and V -clusters and coverings in the structure theory and in the physics of icosahedral quasicrystals.

7 Summary and outlook.

The covering project analyzed here for dual tilings from lattice embedding has the following features:

- (1) *Fundamental domains*: The analysis depends crucially on the notion Def. 2 of a fundamental domain for functions on the position space E_{\parallel} compatible with the tiling.
- (2) *Clusters*: The clusters should be related to the fundamental domain for functions compatible with the tiling. This relation is given for Voronoi or Delone clusters in the 2D Penrose and triangle tilings and must be explored for the dual 3D icosahedral tilings.
- (3) *Center positions and their windows*: The center positions are assumed to be for Voronoi clusters the parallel projected lattice point positions, for Delone clusters the parallel projected hole positions (vertices of Voronoi cells) whose perpendicular projections fall into the window(s) of the tiling. This property is verified for the 1D Fibonacci and A_2 -based tiling and for the dual 2D Penrose and triangle tilings. In all these cases the positions and windows for the centers of the clusters are explicitly determined.
- (4) *Cluster recognition and linkage in the tilings*: In the Fibonacci, the A_2 -based and triangle tiling the clusters appear as collections of full tiles. Their possibly alternative compositions from these tiles and their linkage and overlaps can be unified by appropriate subdivision with or (in case of the A_2 -based tiling) without the use of deflation. For the Penrose rhombus tiling one needs one level of deflation plus the Robinson subdivision to recognize the decagon clusters and to analyze their overlaps and linkage.
- (5) *Covering property*: For Voronoi and Delone clusters in 1D tilings with the assumption (3) on their centers, the covering property can be verified in an elementary way. For the dual 2D tilings the covering property can be shown from the explicit projection and window technique (example in appendix B).
- (6) *Icosahedral clusters*: For the dual 3D icosahedral tilings the Voronoi and Delone clusters are known. The window technique is more involved but available. It must be implemented to relate them to fundamental domains (2), to find the cluster centers and their windows according to (3), to study the covering property (5), and to find the linkage of clusters.

Appendix A: Windows for the pentagonal covering.

We present an independent analysis of the windows for the centers of pentagonal Delone clusters in the tiling (\mathcal{T}^*, A_4) of section 5, using the geometry of [2]. The acute and obtuse triangle tiles t_1, t_2 of this tiling in E_{\parallel} have as windows $w(t_1), w(t_2)$ in E_{\perp} the dual thick and thin Penrose rhombus tiles appearing within the decagonal Voronoi window V_{\perp} . Vertex configurations in the tiling are coded in this window by intersections of the rhombus windows. For the complete list of vertices and windows we refer to [2]. In Fig. 8 we show the collection of those tiles and their windows which together determine the windows for the Delone clusters $D_{\parallel}^a, D_{\parallel}^b$.

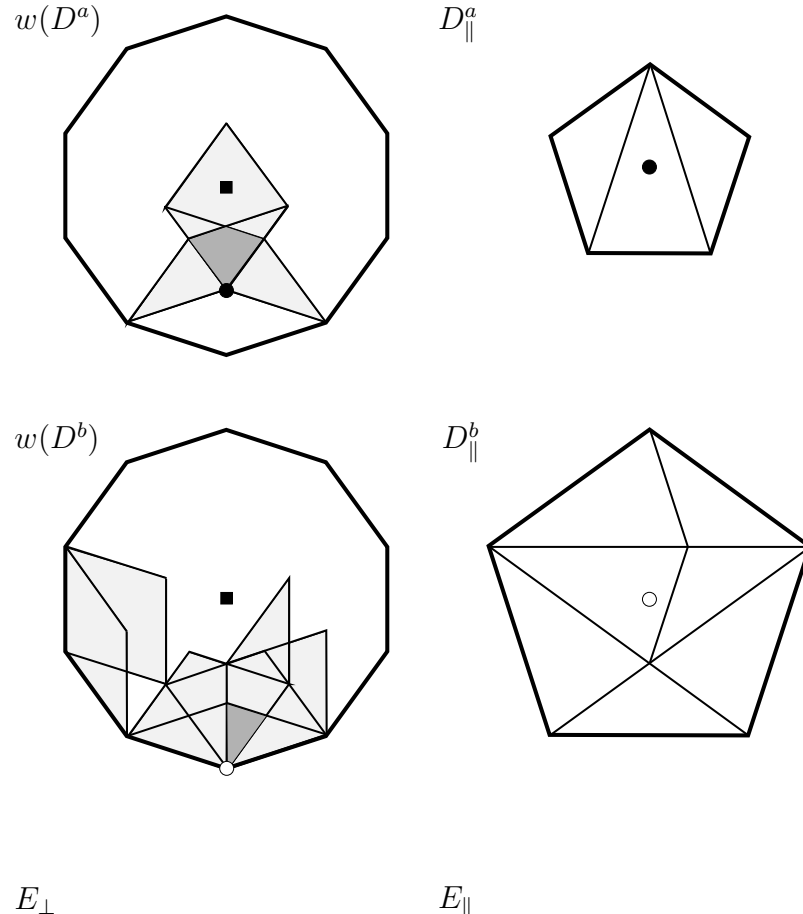


Fig. 8 The windows for the Delone D -clusters of the pentagonal covering of section 5 modulo the point group D_{10} . The small pentagon $D_{\parallel}^a \in E_{\parallel}$ (top, right) is formed from 1 acute triangle t_1 and 2 obtuse triangles t_2 . The

windows for these tiles are 1 thick and 2 thin rhombus tiles $w(t_1), w(t_2)$ in the decagonal window $V_\perp \in E_\perp$ (top, left). Their intersection is the window $w(D^a)$ for a vertex position of the small Delone cluster (grey). The large pentagon $D_\parallel^b \in E_\parallel$ (bottom, right) is formed by 4 acute triangles t_1 and 3 obtuse triangles t_2 . The windows are 4 thick and 3 thin rhombus tiles in the decagonal window (bottom, left). 3 thick and 2 thin rhombus tiles (light grey) intersect in half of the window $w(D^b)$ (grey) which codes the lower vertex position of the large Delone cluster. The remaining acute and obtuse triangle at the upper vertex of the pentagon (right) are forced by the remaining thin and thick rhombus windows shown in the decagon (light grey, left). A reflection in a vertical line both in E_\parallel and E_\perp yields a second version of the cluster D_\parallel^b and the second half of the window $w(D^b)$ shown in Fig. 6.

Appendix B: Covering from projection and windows.

Given a tiling \mathcal{T} and a set of clusters with their center positions, the *covering property* requires that all parts of any tile from the tiling be covered by at least one of the clusters.

For the decagon covering of the Penrose tiling (\mathcal{T}, A_4) the covering property was shown by Gummelt [6]. It was shown in section 4 that the V -clusters for the Penrose tiling coincide with the decagons of Gummelt. The covering property holds by this coincidence. In what follows we give a constructive proof from projections and windows for the covering property of the triangle tiling by pentagonal Delone clusters. A similar constructive proof applies for the Penrose tiling. W

8 Prop. The pentagonal Delone clusters $D_\parallel^a, D_\parallel^b$ with the center positions described in section 5 form a covering of the triangle tiling (\mathcal{T}^*, A_4) .

Proof: The tiles of this tiling are acute or obtuse golden triangles t_1, t_2 , compare Figs. 5, 8 and 9. Their dual windows have the thick and thin Penrose rhombus shape $w(t_1), w(t_2)$ and are located in the decagonal Voronoi window V_\perp . On each rhombus we mark its shallow hole vertex by a full circle. For a fixed orientation of t_1, t_2 , each window $w(t_1), w(t_2)$ appears in the decagon in three shifted positions. These three positions are shown in Fig. 9.

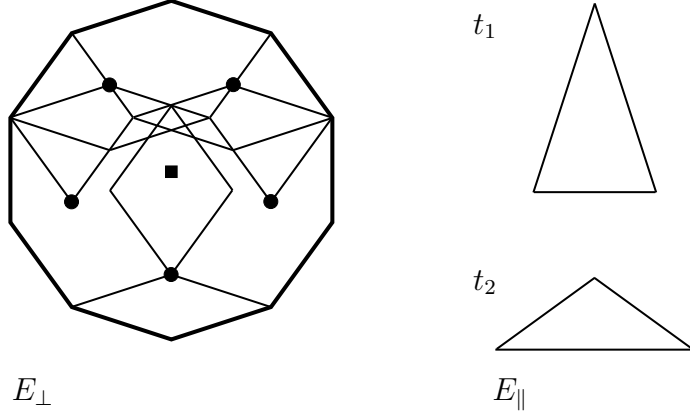


Fig. 9. The acute and obtuse triangle t_1, t_2 (right) of the triangle tiling $(\mathcal{T}, A_4) \in E_{\parallel}$. Their windows $w(t_1), w(t_2)$ in E_{\perp} (left) for fixed orientations are dual thick and thin Penrose rhombus tiles in the decagon V_{\perp} . The shallow hole vertex is marked on each rhombus window by a full circle. Each rhombus window $w(t_i)$ appears in three shifted positions.

For all other orientations under the action of the point group D_{10} in E_{\parallel} , the windows transform under the corresponding action of D_{10} but now in E_{\perp} [2]. For example under a rotation of the tiles by $2\pi/5$ their windows must be rotated by $4\pi/5$.

Consider next the Delone clusters $D_{\parallel}^a, D_{\parallel}^b$ of section 5 with their composition out of 3 and 7 triangle tiles respectively. In appendix A Fig. 7 we give for both clusters with fixed orientation the collection of the 3 and 7 rhombus windows $w(t_1), w(t_2)$ within V_{\perp} . A comparison of the left-hand sides of Figs. 7 and 8 for E_{\perp} shows: Any single rhombus window $w(t_i)$ for a single triangle tile t_i in the 3 possible shifted positions of Fig. 8 can be brought modulo D_{10} into coincidence with at least one rhombus window $w(t_j)$ from the collection for D_{\parallel}^a or D_{\parallel}^b given in Fig. 7. In E_{\parallel} this implies that for any triangle tile $t_i \in (\mathcal{T}, A_4)$ one can construct at least one Delone cluster D_{\parallel}^a or D_{\parallel}^b that covers this tile. \square

References

- [1] Arnold V I, *Remarks on quasicrystallic symmetries*, Phys. **D 33** (1988) 21-25
- [2] Baake M, Kramer P, Schlottmann M and Zeidler D, *Planar patterns with fivefold symmetry as sections of periodic structures in 4-space* Int. J. Mod. Phys. **B 4** (1990) 2217-68
- [3] Burkov S, *Enforcement of matching rules by chemical ordering in the decagonal $AlCuCo$ quasicrystal*, Phys. Rev. **B 47** (1993) 12325
- [4] Grünbaum B and Shepard G C, *Tilings and Patterns*, Freeman, New York 1987, 562
- [5] Conway J H and Sloane N J A, *Sphere Packings, Lattices and Groups*, Springer, New York 1988, 31-36
- [6] Gummelt P, *Penrose tilings as coverings of congruent decagons*, Geometriae Dedicata **62** (1996) 1-17
- [7] Janot C, *Conductivity in quasicrystals via hierarchically variable-range hopping*, Phys. Rev. **B 53** (1996) 181-189
- [8] Katz A and Gratias D, *A geometric approach to chemical ordering in icosahedral structures*, J. of Non-Cryst. Solids 153,154 (1993) 187-195
- [9] Katz A and Gratias D, *Chemical order and local configurations in $AlCuFe$ -type icosahedral phase*, in: Proc. Int. Conf. Quasicrystals, eds. C. Janot and R. Mosseri, World Scientific, Singapore (1995) 164-167
- [10] Kramer P and Papadopolos Z, *Symmetry concepts for quasicrystals and noncommutative crystallography*, in: Proc. ASI Aperiodic Long Range Order, Waterloo 1995, ed. R.V. Moody, Kluwer, New York 1995, 307-330
- [11] Kramer P, *Atomic order in quasicrystals is supported by several unit cells*, Mod. Phys. Lett. **B 1** (1987) 7-18
- [12] Kramer P, *Space-group theory for a non-periodic icosahedral quasilattice*, J. Math. Phys. **29** (1988) 516-524
- [13] Kramer P and Schlottmann M, *Dualization of Voronoi domains and klotz construction: a general method for the generation of proper space filling*, J. Phys. **A 22** (1989) L1097-L1102

- [14] Kramer P, Papadopolos Z and Zeidler D, *Symmetries of icosahedral quasicrystals*, in: *Symmetries in Science V*, eds. B. Gruber, L. C. Biedenharn and H. D. Doebner, Plenum, New York (1991) 395-427
- [15] Kramer P, Quandt A, Schneider Th and Teuscher H, *Simulation of Mössbauer absorption spectra for decagonal AlCuCo*, Phys. Rev. **B 55** (1997) 8793-8800
- [16] Jeong H-C and Steinhardt P J, *Constructing Penrose-like tilings from a single prototile and the implications for quasicrystals*, Phys. Rev. **B 55** (1997) 3520-3532
- [17] Steinhardt P J and Jeong H-C, *A simpler approach to Penrose tilings with implications for quasicrystal formation*, Nature **382** (1996) 431-433
- [18] Steinhardt P J, Jeong H-C, Saitoh K, Tanaka M, Abe E and Tsai A P, *Experimental verification of the quasi-unit cell model of quasicrystal structure*, Nature **396** (1998) 55-57
- [19] Urban K W, *From tilings to coverings*, Nature **396** (1998) 14-15